WARSAW UNIVERSITY OF TECHNOLOGY Index 351733
FACULTY OF CIVIL ENGINEERING
COMMITTEE FOR CIVIL AND WATER ENGINEERING
POLISH ACADEMY OF SCIENCES ISSN 1230-2945

DOI: 10.24425/ace.2023.146078

ARCHIVES OF CIVIL ENGINEERING

Vol. LXIX ISSUE 3 2023

pp. 239 –251

Research paper

Cracking control technique for continuous steel-concrete composite girders under negative bending moment

Min Cai[1], Wenjie Li[2], Zhiyong Wan[3], Jianjun Sheng[4], Juliang Tan[5], Chao Ma[6]

Abstract: Continuous steel-concrete composite girder can fully utilize material strength and possess large spanning ability for bridge constructions. However, the weak cracking resistance at the negative bending moment region of the girder seriously harms its durability and serviceability. This paper investigates practical techniques to improve the cracking performance of continuous steel-concrete composite girders subjected to hogging moment. A real continuous girder was selected as the background bridge and introduced for numerical analysis. Modeling results show that under the serviceability limit state, the principle stress of concrete slabs near the middle piers of the bridge was far beyond the allowable material strength, producing a maximum tensile stress of 10.0 MPa. Approaches for strengthening concrete decks at the negative moment region were developed and the effectiveness of each approach was assessed by examing the tensile stress in the slabs. Results indicate that the temporary counterweight approach decreased the maximum tensile stress in concrete slabs by 22%. Due to concrete shrinkage and creep, more than 65% of the prestressed compressive stresses in concrete slabs were finally dispersed to the steel beams. A thin ultra-high performance concrete (UHPC) overlay at the hogging moment region effectively increased the cracking resistance of the slabs, and practical engineering results convicted the applicability of the UHPC technique.

Keywords: continuous steel-concrete composite girder, hogging moment, cracking performance, strengthening approach, ultra-high performance concrete

[1]MSc., Senior engineer, Guangdong Highway Construction Co., LTD, 510623 Guangzhou, China, e-mail: 9990430@qq.com, ORCID: 0009-0006-1279-5375

[2]Senior engineer, Guangdong Yunmao Expressway Co. Ltd, 525346 Guangzhou, China, e-mail: 442113935@qq.com, ORCID: 0009-0007-6410-7252

[3]PhD. candidate, Professor senior engineer, Guangdong Communication Planning & Design Institute Co., Ltd, 510507 Guangzhou, China, e-mail: 1095801967@qq.com, ORCID: 0009-0003-6375-9516

[4]Senior engineer, Guangdong Highway Construction Co., LTD, 510623 Guangzhou, China, e-mail: 8440241@qq.com, ORCID: 0009-0002-3126-0625

[5]Senior engineer, Guangdong Communication Planning & Design Institute Co., Ltd, 510507 Guangzhou, China, e-mail: 3011905633@qq.com, ORCID: 0009-0007-6611-9978

[6]Engineer, Guangdong Highway Construction Co., LTD, 510623 Guangzhou, China, e-mail: 1712913101@qq.com, ORCID: 0009-0005-2035-7706

1. Introduction

During the past decades, steel girder bridges, such as steel box-girder bridges, steel truss-girder bridges, and steel-concrete composite girder bridges, have been widely used in expressway bridge constructions [1–5]. The steel-concrete composite girder bridge, retaining concrete slabs in the compression area and steel beam in the tension area and integrating the two parts via shear connectors, exhibits outstanding efficiency in utilizing the strength of the constitutive materials. Since the steel beam at the lower side of the composite girder carries most of the permanent and traffic loads, the upper concrete deck in compression is usually thin. It consumes few natural resources, making the composite girder bridge more environment-friendly than traditional steel-reinforced concrete bridges. So far, many steel-concrete composite girder bridges have been constructed worldwide [4–8].

With the intensive establishment of steel-concrete composite girder bridges, the merits of such structures, including simple structural arrangement, easy construction and maintenance, and good spanning ability, have been gradually convicted [9, 10]. Noticeably, the advantage of the composite girder relies on the upper concrete deck in compression and the lower steel beam in tension. However, near the middle pier of the continuous steel-concrete composite girder, the hogging moment violates this law. It subjects the upper concrete deck slab to tension and the bottom steel beam to compression [11–13]. Under the hogging moment, the concrete deck with low tensile strength would inevitably crack and bring poor durability and low safety margin, making the deck slab at the region easy to deteriorate during the bridge operation [14].

Many researchers and engineers have tried to solve the cracking problem for continuous steel-concrete composite girder bridges. Various approaches have been proposed to strengthen the concrete decks at the negative bending moment region [15–19]. However, existing approaches mostly concentrate on the single crack-controlling technique, which cannot completely solve the cracking problem of the continuous composite girder bridge exposed to severe load conditions and harsh environments [20–23]. The easy cracking of the hogging moment zone has seriously prevented the further application of continuous steel-concrete girder bridges. Practical approaches to improving the cracking performance of concrete decks under hogging moment are to be investigated.

This paper focuses on practical techniques to improve the cracking performance of continuous steel-concrete composite girder bridges under hogging moment. A real continuous steel-concrete composite girder bridge under construction was briefly introduced for numerical analysis. Several approaches for strengthening the concrete decks at the negative moment region were developed, and the effectiveness of each approach was assessed by analyzing the performance of the decks. Based on the results from the models and engineering practice, an efficient technique that uses a thin layer of UHPC on the top of normal concrete substrates to strengthen the cracking performance of concrete decks at the negative bending moment region of the continuous steel-concrete composite girder was proposed. The usefulness of the UHPC overlay is examined through engineering verification. The achievements of this study can provide a reference for future application of the proposed approach.

2. Porotype bridge and performance evaluation

2.1. Prototype bridge

The selected continuous steel-concrete composite girder is the Gaotai Bridge, part of the Yunmao Expressway, under construction in the Guangdong province of China. Figure 1 shows the configuration and arrangement of the Gaotai Bridge. As can be seen, the prototype bridge had a span arrangement of 17×40 m, an overall deck width of 12.5 m, a longitudinal slope of 2.5%, and a lateral deck slope of 2.0%. The design vehicle speed and seismic peak acceleration of the Gaotai Bridge were 100 km/h and 0.05 g, respectively. The maximum height of the thin-walled hollow piers was 68 m.

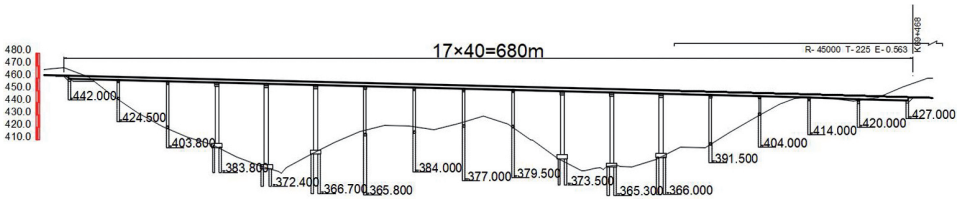

(a) the overall arrangement of the Gaotai Bridge

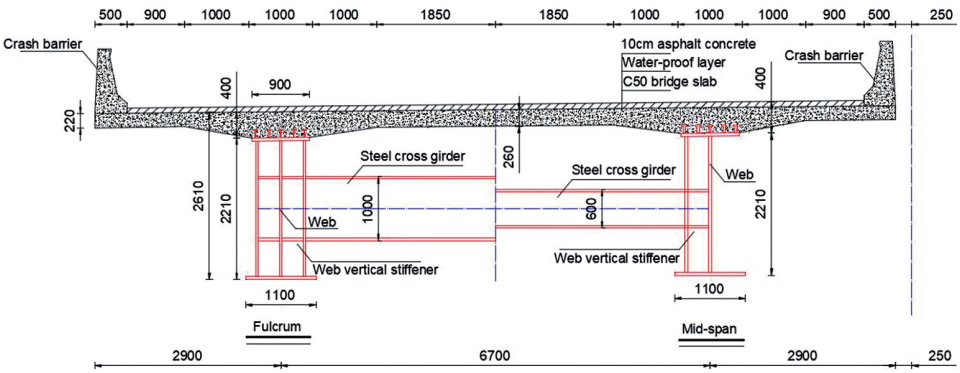

(b) cross-section of the bridge

Fig. 1. Configuration of Gaotai Bridge (cm)

The continuous girder bridge comprises a solid deck fabricated using C55 normal concrete, a pair of parallel I-shaped steel beams fabricated using Q345C grade steel, and several pieces of headed steel studs connecting the concrete deck and steel beams. The concrete deck thickness near the steel flanges and the bridge longitudinal axis was 0.4 m and 0.26 m, respectively. Reinforcement bars in the deck slabs were made of HRB400 grade steel (with a nominal yield strength of 400.0 MPa), which were longitudinally arranged in two layers. The diameter and distribution intervals were 28.0 mm and 120.0 mm for the top layer reinforcement bars, respectively. The diameter and distribution intervals were 25.0 mm and 100.0 mm for the bottom layer reinforcement bars, respectively. The I-shaped

steel beam had an overall depth of 2.2 m, a top flange width of 0.9 m, and a bottom flange width of 1.1 m. Steel diaphragms were welded to the parallel beams' steel webs to ensure the girder's stability. All steel members were fabricated in a factory and delivered to the construction site. After the completion of the piers, the I-shaped steel beams were assembled through incremental launching. The concrete slabs were prefabricated in segments and then assembled through cranes.

2.2. Finite element model

Based on the *ANSYS 15.0* code, a solid nonlinear finite element (FE) model was established for the Gaotai Bridge to assess the performance of the concrete decks at the hogging moment region. The FE model consists of a concrete slab, a pair of I-shaped steel beams, and prestressed strands. The constitutive model of the C55 concrete and Q345C steel is defined based on the stress-strain relationship provided in the code [24]. All concrete slabs are modeled using Solid 65 elements, while the steel beams and prestressed tendons are modeled using Shell 63 and Link 8 elements, respectively. All nodes at the interface between concrete decks and steel beams are coupled together, considering the strong restraints of the headed steel studs in the actual girder. In order to model the influence of concrete cracking on the stresses, the element death function was activated when the stress or strain in the Solid 65 element reached its permitted values. The application of prestressed tendons is realized by applying initial strains to the strands. According to the element sensitivity analysis results, the stress obtained from the composite beam models significantly varied with the element meshing size, and the stress became stable after the element size of concrete and steel approached 50 mm and 25 mm, respectively. Consequently, the concrete slab has meshed using element sizes of 50 mm. The element sizes selected for the steel beam and prestressed tendons are 25.0 mm. The established FE model of the Gaotai Bridge is shown in Fig. 2.

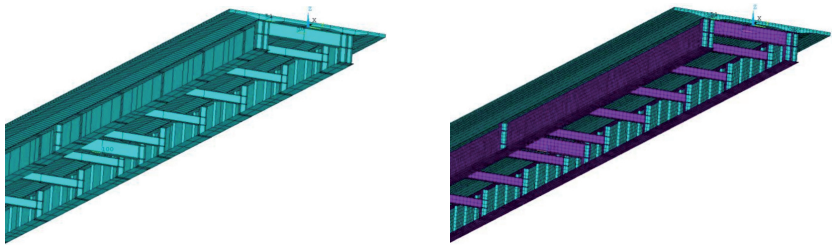

(a) geometric model (b) element mesh model

Fig. 2. Finite element model of Gaotai Bridge

As shown in Fig. 3, the vehicle load level-I, composed of a standard uniform load (q_k) and a standard concentrated load (P_k), is applied to the FE models. The concentrated load P_k is indirectly applied to the composite girder to avoid stress concentrations. The P_k is applied to a referring node adjacent to the expected loading point, and the referring node

is coupled with the concrete nodes at the region. The arrangement of the loads is based on the principle of generating maximum negative bending moments for the girder. According to the Chinese code [25], the q_k is a constant parameter of 10.5 kN/m. The value of P_k is associated with the calculated span and can be determined from Table 1. Considering the influence of the multi-lanes on the deck, a vehicle load reduction coefficient of $\zeta_q = 1.843$, suggested by the code [25], is employed for calculation.

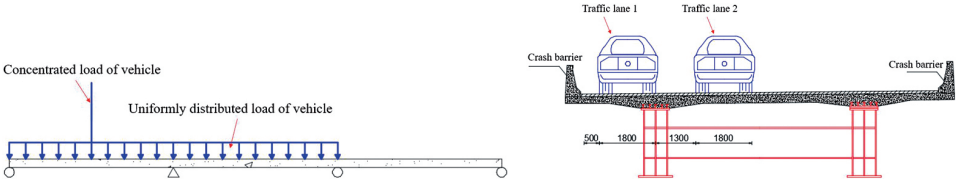

(a) distribution of standard vehicle loads (b) arrangement of standard lanes

Fig. 3. Most critical load arrangement of the girder (m)

Table 1. Determination of concentrated load (P_k)

Calculation span L_0 (m)	$L_0 \leq 5$	$5 < L_0 \leq 50$	$L_0 \geq 50$
P_k (kN)	270	$2 \times (L_0 + 130)$	360

2.3. Performance evaluation

The stresses in the concrete decks under the "standard load combination" and "short-term load combination" are achieved using the FE models. Figure 4 presents a summary of the results. As seen, concrete decks above middle piers are exposed to significant tensile stresses due to negative bending moments. Under the "standard load combination", the tensile stress in concrete decks is mostly between 5.0 MPa and 8.0 MPa, giving a maximum value of 10.0 MPa. On the other hand, the "short-term load combination" generates tensile

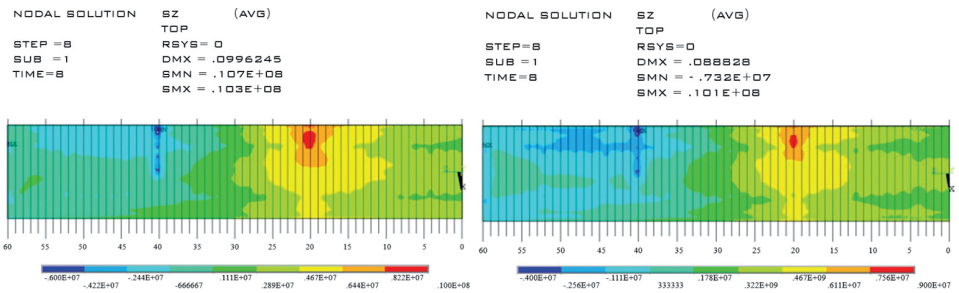

(a) standard load combination (b) short-term load combination

Fig. 4. Stresses in concrete decks (MPa)

stresses in concrete decks between 4.0 MPa and 7.0 MPa, showing a peak stress of 9.0 MPa. The tensile stresses at the negative moment region are far beyond the allowable tensile strength of the concrete. It is essential to explore effective ways to ensure durability and serviceability at the negative bending moment region of the bridge.

3. Approaches and feasibility assessment

The purpose of strengthening concrete decks at the negative moment region is to minimize the tensile stress and crack width. Based on the evaluation of the Gaotai Bridge, approaches to improve the concrete decks of the bridge are introduced and verified.

3.1. Strengthening approaches

3.1.1. Optimizing concrete fabrication Sequence

For the investigated continuous steel-concrete composite girder bridge, tensile stress in concrete slabs is primarily determined by the negative bending moments. By adjusting the concrete slab fabrication sequence, it is practical to reduce the negative moment caused by the permanent loads of the bridge. Compared to the one-time casting of all concrete slabs, installing the concrete slabs in stages brings a relatively small hogging moment above the middle piers. As shown in Fig. 5, after placing the I-shaped steel beams, fabricate concrete slabs at the positive bending moment region of the girder first and then fabricate the concrete slabs near the piers.

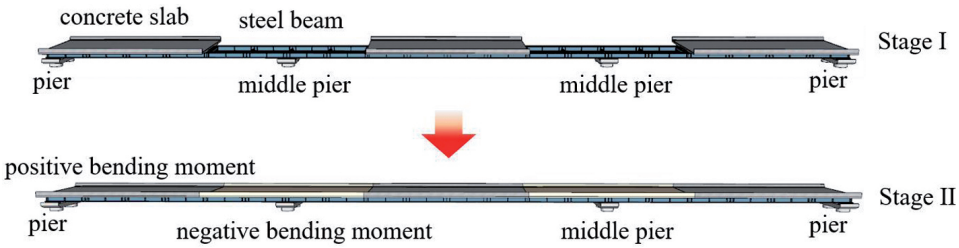

Fig. 5. Adjustment of the slab fabrication sequence

3.1.2. Involving temporary counterweight

After completing the construction of concrete slabs at the positive bending moment region, applying a temporary counterweight at the middle point of each span may also reduce the hogging moment from the permanent loads. As shown in Fig. 6, applying additional temporary loads to the girder's middle span, and then removed the counterweight after the slabs at the hogging moment region were fabricated. Removing the temporary counterweight would expose concrete slabs at the hogging moment region to axial compression due to the steel beams' resilience at the girder's middle span.

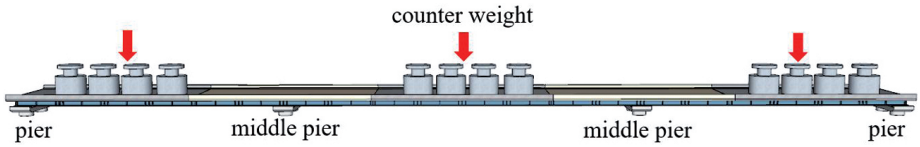

Fig. 6. Application of temporary counterweight at positive moment region

3.1.3. Applying Prestressed Tendons

Applying prestressed tendons to concrete slabs at the negative bending moment region is a conventional method for crack control in composite girder bridges. The steel strands are axially embedded in concrete slabs near the middle piers, and the strands are tensioned after the completion of the concrete slabs and steel beams. Due to the combined effects between the steel and concrete members, part of the prestressed loads would flow into the steel beam, resulting in significant stress loss for the concrete slabs. Moreover, the development of concrete shrinkage and creep during bridge operation would also decrease the compressive stress in the concrete, exposing the slab at the negative bending moment region to a high risk of cracking [10]. Consequently, it is critical to provide sufficient steel strands to the hogging moment region of the bridge.

3.1.4. Employing UHPC overlay

Ultra-high performance concrete (UHPC) is a new cement-based composite material with super-high strength, high toughness, and remarkable durability [23]. The tensile strength of UHPC is very high and reaches up to 5 to 10 times that of traditional concrete. With such merits, the UHPC has recently been widely used in bridge construction. For the investigated Gaotai bridge, applying UHPC at the negative bending moment zone may improve the cracking resistance of the slabs. As shown in Fig. 7, replace the normal concrete slab's top layer near the middle piers with a UHPC overlay, and the normal concrete substrate is connected with the top UHPC through interfacial shear steel rebars. The thin UHPC layer directly resists the maximum tensile stress caused by the hogging moment.

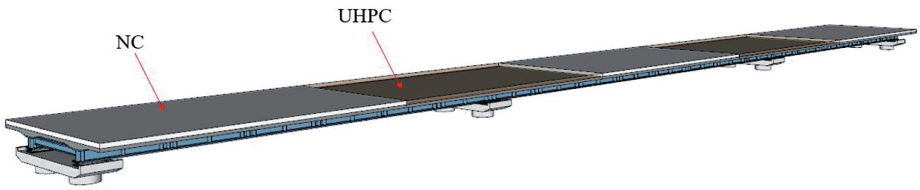

Fig. 7. Employment of UHPC overlay at hogging moment region

3.2. Feasibility assessment

The feasibility of the above approaches for the investigated structure is evaluated and discussed based on the established FE models.

3.2.1. Evaluation of optimizing concrete fabrication Sequence

Stress obtained from the model with an optimized concrete fabrication sequence is presented in Fig. 8. As can be seen, the maximum concrete tensile stress occurs at the top surface of the slabs near the middle piers. Under the permanent and vehicle loadings, the maximum tensile stress in concrete slabs is 6.23 MPa, which is 34.5% smaller than that obtained from the model with a one-time concrete cast. Due to the unbalanced arrangement of the vehicle loadings, it is noted that the peak stresses unsymmetrically distribute along the deck axis. Although adjusting the concrete construction sequence reduced the concrete stress, the large tensile stress in the slabs still exposed the girder to inevitable cracking under the hogging moment.

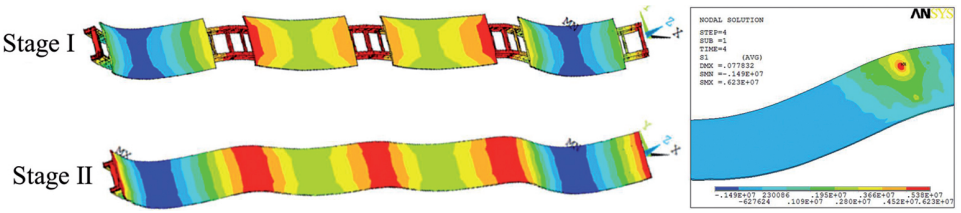

Fig. 8. Tensile stresses in concrete slabs

3.2.2. Evaluation of involving temporary counterweight

A concentrated load of 900 kN is applied to the middle point of each span, and the temporary load is removed after completing the concrete near the middle piers. A summary of the structural responses of the girder under the loadings is presented in Table 2. As can be seen, after completion of the slab at the positive bending moment region, introducing a load of 900 kN to the mid-span slightly increased the girder deflection by 10.5% and the maximum tensile stress of the steel beam by 16.0%. In comparison, the maximum concrete tensile stress near slab edges is drastically increased from 0.18 MPa to 2.86 MPa. This is mainly caused by the stress concentrations from the applied temporary loads. After the bridge's construction, the maximum concrete tensile stress at the hogging moment region is reduced by 22.6% compared to the counterpart without the temporary load.

Table 2. Structural response of the girder with a temporary counterweight

Stage	Location	Item	Without counter-weight	With counter-weight
Completion of concrete at positive moment zone	At mid-span point	Deflection (cm)	5.77	6.36
		Concrete stress (MPa)	0.18	2.86
		Steel stress (MPa)	130.92	151.86
Completion of the entire bridge	Over middle pier	Concrete stress (MPa)	6.23	4.82

3.2.3. Evaluation of applying prestressed tendons

In the analytical model, the prestressed tendons installed at the hogging moment region produced a uniform initial compressive stress of 10.0 MPa in the concrete slab. The distribution of stresses at the hogging moment region is presented in Fig. 9. Due to the existence of concrete shrinkage and creep, the residue compressive stress in concrete slabs is about 3.5 MPa after the bridge operated for ten years (~3650 days), showing a stress decrease of 65%. In comparison, the stress in the steel beam is enlarged by 46.0 MPa due to the shrinkage and creep effect. Apparently, using prestressed tendons to increase the cracking resistance of the concrete slabs is a non-ideal for the bridge, in addition to the inconvenient installation of steel strands on site.

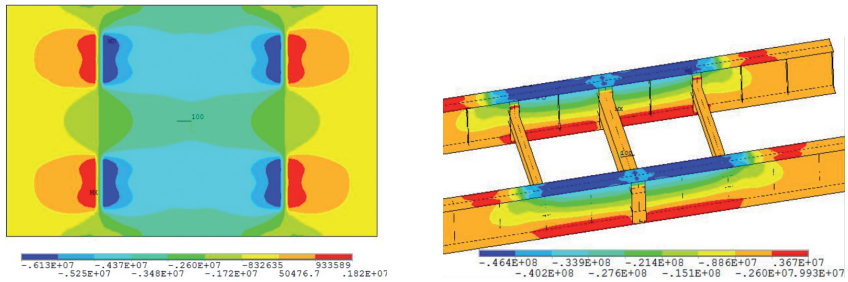

(a) concrete slab (b) steel beam

Fig. 9. Stress distribution of steel and concrete members

3.2.4. Evaluation of employing UHPC overlay

To examine the feasibility of using UHPC at the negative bending moment region, models with a UHPC slab and a normal concrete slab topped by 10 cm-thick UHPC overlay, respectively, are established. Figure 10 shows the stress in concrete slabs near the middle piers. As can be seen, the maximum tensile stress in the UHPC slab and UHPC overlaid normal concrete slab is very close and ranges from 7–8 MPa, which is lower than

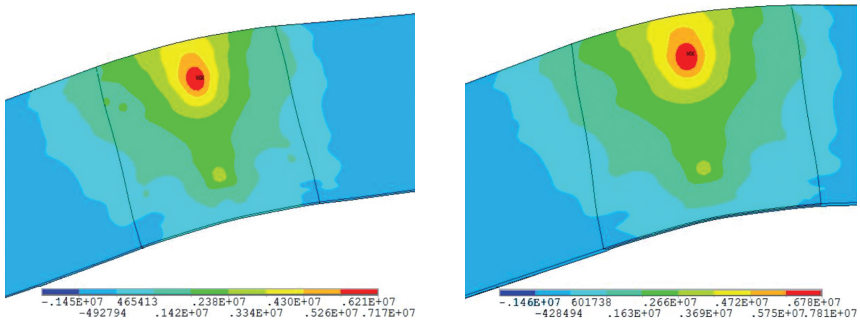

(a) UHPC slab (b) slab with a 10 cm-thick UHPC overlay

Fig. 10. Stress distribution in concrete slabs

the allowable tensile strength of the material. Similar stresses indicate that even a thin layer of UHPC topping on normal concrete can prevent cracking under the negative bending moment. By checking the stresses obtained from the model using a normal concrete slab, it is noted that the model with a UHPC slab produces comparatively larger stress than the former. This can be explained by the more loads carried by the UHPC slab due to the large elasticity modulus of the UHPC.

4. Engineering verification

To furtherly examine the usefulness of the approaches above, the Gaotai Bridge was used for practical verification. Since the stress concentration caused by the temporary counterweight approach and prestressed tendons harms the girder's cracking performance, as shown in Fig. 11, strengthening approaches, including the optimization of the concrete slab fabrication sequence and the employment of UHPC overlay, were adopted in the construction of the Gaotai bridge. The thickness of the UHPC layer is 10 cm, and the diameter of shear steel bars at the UHPC overlay-to-normal concrete substrate interface is 12.0 mm. The UHPC was cast after the normal concrete substrate was cured for 7 days. The mix proportion and mechanical properties of the UHPC material used in the prototype bridge are presented in Table 3.

Fig. 11. UHPC overlaid concrete slab of prototype bridge

The cracking condition of the Gaotai Bridge was recorded. The results were measured from the surfaces of the concrete slabs at the hogging moment region. After completion of the UHPC overlay and before constructing asphalt pavement, the composite girder was preloaded to generate a target maximum negative bending moment above the intermediate supports, and it was shown that the UHPC strains recorded by the vibrating wire strain gauge above the intermediate supports were small and no visible cracking was observed at the region. The strain gauges were retained and well protected during the exploitation of the bridge, and the monitored strains were throughout within the cracking strength of the material. Besides, periodic detections of the flange side surfaces indicated no cracking to the composite deck slabs even after the bridge opened for around three years. The

Table 3. Mix proportions and mechanic properties of UHPC

Mix proportion						Mechanical properties (MPa)			
Cement	Silica fume	Quartz powder	Quartz sand	Superplasticizer	Steel fiber	Compressive strength	Primal strength	Tensile strength	Young's modulus
1.0	0.25	0.10	1.10	0.03	2.0%	122	101	11.5	44.0×10^3

favorable practical results indicate that the strengthening approaches effectively improved the cracking resistance of the structure. However, the referred engineering practice did not consider the influence of different interface treatments between the UHPC overlay and concrete substrates. As such, more tests on the composite beams with UHPC at the negative bending moment zone are needed to examine the approach's feasibility further.

5. Conclusions

Based on the construction of a real continuous steel-concrete composite girder bridge in China, effective techniques to improve the cracking performance of the bridge under hogging moment are analyzed and discussed. The main conclusions are drawn as follows:

1. Under the serviceability limit state, concrete decks at the middle piers were exposed to a high risk of cracking due to the negative bending moment. It is critical to adopt effective strengthening approaches to ensure the long-term durability and serviceability of the bridge.
2. Four types of different slab strengthening approaches were introduced. The maximum tensile stress of the bridge using the optimized fabrication sequence method is decreased by 34.5% compared to those with the slabs cast in one-time. The maximum concrete stress is reduced by 22.6% compared to that without the counterweight load.
3. Applying prestressed tendons at the negative moment region can effectively decrease concrete tensile stress in the short term. However, the development of concrete creep and shrinkage in the long term significantly decreased the applied compressive stresses in the concrete, exposing the slab at the region to inevitably cracking.
4. Using a thin layer of UHPC on the top of a normal concrete slab can effectively prevent the slab from cracking at the negative moment region of the bridge. The continuous steel-concrete composite girder using an optimized concrete fabrication sequence and a 10 cm-thick UHPC overlay at the negative bending moment zone of the girder exhibit good cracking performance and superior durability.

Acknowledgements

The authors express their sincere gratitude for the financial support provided by the Science and Technology Project of Guangzhou, China (Grant # 202102020652).

References

[1] J. Nie, et al., "Advances of research on steel-concrete composite bridges", *China Civil Engineering Journal*, vol. 45, no. 6, pp. 110–122, 2012, doi: 10.15951/j.tmgcxb.2012.06.003.

[2] S. He, et al., "Structural performance of perforated steel plate-CFST arch feet in concrete girder-steel arch composite bridges", *Journal of Constructional Steel Research*, vol. 201, art. no. 107742, 2023, doi: 10.1016/j.jcsr.2022.107742.

[3] B. Grzeszykowski and E. Szmigiera, "Nonlinear longitudinal shear distribution in steel-concrete composite beams", *Archives of Civil Engineering*, vol. 65, no. 1, pp. 65–82, 2019, doi: 10.2478/ace-2019-0005.

[4] H.H. Xin, A. Mosallam, et al., "Analytical and experimental evaluation of flexural behavior of FRP pultruded composite profiles for bridge deck structural design", *Construction and Building Materials*, vol. 150, pp. 123–149, 2017, doi: 10.1016/j.conbuildmat.2017.05.212.

[5] T. Keller, et al., "Quasi-static and fatigue performance of a cellular FRP bridge deck adhesively bonded to steel girders", *Composite Structures*, vol. 70, no. 4, pp. 484–496, 2005, doi: 10.1016/j.compstruct.2004.09.028.

[6] J.W. Wang, et al., "Stability monitoring method of UHPC spherical hinge horizontal rotation system", *Archives of Civil Engineering*, vol. 68, no. 3, pp. 601–616, 2022, doi: 10.24425/ace.2022.141905.

[7] H.H. Xin, et al., "Material-structure integrated design optimization of GFRP bridge deck on steel girder", *Structures*, vol. 27, pp. 1222–1230, 2020, doi: 10.1016/j.istruc.2020.07.008.

[8] L.Y. Kou, "Research and perspective of slip property of composite steel-concrete beams", *Construction and Design for Engineering*, vol. 11, pp. 43–46, 2010, doi: 10.3969/j.issn.1007-9467.2010.11.013.

[9] C.Y. Shao, "Development and application prospect of combined structural bridge", *Urban Roads Bridges and Flood Control*, vol. 9, pp. 11–15+260+6, 2016, doi: 10.16799/j.cnki.csdqyfh.2016.09.003.

[10] S. He, et al., "Experimental study on flexural performance of HSS-UHPC composite beams with perfobond strip connectors", *Journal of Structural Engineering*, vol. 148, no. 6, art. no. 04022064, 2022, doi: 10.1061/(ASCE)ST.1943-541X.0003366.

[11] Y.J. Liu, et al., "Transverse moment of steel- concrete composite twin I-girder bridge deck", *Journal of Chang'an University*, vol. 42, no. 6, pp. 1–11, 2022, doi: 10.19721/j.cnki.1671-8879.2022.06.001.

[12] J.S. Fan, et al., "Effects of slips on load-carrying capacity of composite beams under negative bending", *Engineering Mechanics*, *vol.* 22, n. 3, pp. 177–182, 2005, doi: 10.3969/j.issn.1000-4750.2005.03.031.

[13] S.H. He, et al., "Flexural performance of HSS-UHPC composite beams with perfobond strip connectors", *Journal of Traffic and Transportation Engineering*, vol. 22, no. 6, pp. 143–157, 2022, doi: 10.19818/j.cnki.1671-1637.2022.06.009

[14] J. Li, et al., "Simulated test research on mechanical performance of steel-concrete composite beam of prestress construction", *Journal of Railway Science and Engineering*, vol. 2, pp. 14–19, 2001, doi: 10.19713/j.cnki.43-1423/u.2001.02.003.

[15] J.L. Xiao, et al., "Flexural behavior of wet joints in steel-UHPC composite deck slabs under hogging moment", *Engineering Structures*, vol. 252, art. no. 113636, 2022, doi: 10.1016/j.engstruct.2021.113636.

[16] S.H. He, et al., "Evaluation of shear lag effect in HSS-UHPC composite beams with perfobond strip connectors: Experimental and numerical studies", *Journal of Constructional Steel Research*, vol. 194, art. no. 107312, 2022, doi: 10.1016/j.jcsr.2022.107312.

[17] Y. Xu, et al., "Shear behavior of flexible-sleeve perfobond strip connectors: Experimental and analytical studies", *Engineering Structure*s, vol. 264, art. no. 114380, 2022, doi: 10.1016/j.engstruct.2022.114380.

[18] J.F. An, et al., "Factors affecting cracking and crack control measures of steel-concrete composite girder bridge", *Journal of Nanjing Tech University (Natural Science Edition)*, vol. 42, no. 3, pp. 389–398, 2020, doi: 10.3969/j.issn.1671-7627.2020.03.016.

[19] H.Y. Wu, "Research on control measures for cracks in hogging moment area of curved composite beam", *Northern Communications*, vol. 4, pp. 39–43+46, 2018, doi: 10.15996/j.cnki.bfjt.2018.04.011.

[20] D. Chen, et al., "Research on control measures for cracks in hogging moment area of composite beam using industrial construction method", *Shanghai Highway*s, vol. 3, pp. 51–53+57+4, 2019, doi: 10.3969/j.issn.1007-0109.2019.03.013.

[21] C. Shim and C. Lee, "Crack width control of precast deck loop joints for continuous steel-concrete composite girder bridges", *Advances in Concrete Construction*, vol. 10, no. 1, pp. 21–34, 2020, doi: 10.12989/acc.2020.10.1.021.

[22] S.H. Long, et al., "Review on crack control in hogging moment zone of steel-concrete composite girder bridge", *Jiangxi Building Materials*, vol. 9, pp. 21–23, 2021, doi: 10.3969/j.issn.1006-2890.2021.09.009.

[23] S.H. He, et al., "Investigation on interfacial anti-sliding behavior of high strength steel-UHPC composite beams", *Composite Structure*s, vol. 316, art. no. 117036, 2023, doi: 10.1016/j.compstruct.2023.117036.

[24] GB 50010-2010 Code for Design of Concrete Structures. China Industry Press, 2015.

[25] JTG D60-2019 General Code for Highway Bridges and Culverts. China Communications Press, 2020.

Received: 2023-05-03, Revised: 2023-06-09